

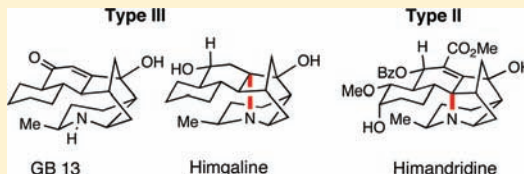
# Progress toward the Syntheses of (+)-GB 13, (+)-Himgaline, and Himandridine. New Insights into Intramolecular Imine/Enamine Aldol Cyclizations

David A. Evans,\* Drew J. Adams, and Eugene E. Kwan

Department of Chemistry & Chemical Biology, Harvard University, Cambridge, Massachusetts 02138, United States

## Supporting Information

**ABSTRACT:** A full account of our total synthesis of the galbulimima alkaloids GB 13 and himgaline is provided. Using a strategy adapted from the proposed biosynthesis of the GB alkaloid family, a linear precursor underwent successive intramolecular Diels–Alder, Michael, and imine aldol cyclizations to form the polycyclic alkaloid core. We now show that modification of this strategy can also deliver an advanced intermediate en route to the related alkaloid himandridine. The success of the key imine aldol cyclization is acutely sensitive to substrate structure and solvent, including a case in which cyclization was spontaneous in protic solvents. A detailed computational investigation of the course of the reaction closely correlates with, and suggests a rationale for, the observed patterns of imine aldol reactivity.



## INTRODUCTION

**Background.** The galbulimima alkaloids comprise 28 polycyclic isolates of *Galbulimima belgraveana*, a rare rain forest tree found in Papua New Guinea and northern Australia (Figure 1).<sup>1</sup> Native tribes have used bark extracts from this tree

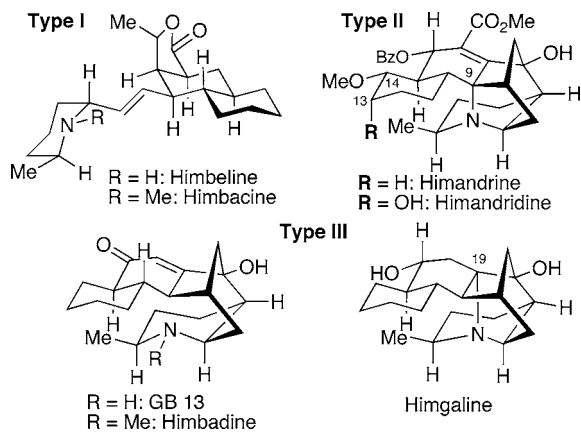


Figure 1. Representative GB alkaloids.

for medicinal and spiritual purposes,<sup>2</sup> and the Type I GB alkaloid himbacine has been demonstrated to have potent, selective antimuscarinic activity.<sup>3</sup> Largely as a result of its potentially therapeutic biological properties,<sup>4</sup> multiple syntheses of himbacine<sup>5</sup> and its simplified analogs<sup>6</sup> have appeared.

The Type II and Type III GB alkaloids have also attracted the attention of several research groups as a result of their complex polycyclic architectures. In addition to the racemic synthesis of GB 13 reported by Mander prior to the outset of this work,<sup>7a</sup> both Movassaghi<sup>7b</sup> and Chackalamannil<sup>7c</sup> have reported approaches to GB 13. Chackalamannil's investigation

also described the conversion of GB 13 to the related Type III alkaloid himgaline. These syntheses led to a revision of the absolute configuration of the Type III alkaloids. More recently, an X-ray crystallographic analysis reported by Mander supported revision of the Type II alkaloids.<sup>8</sup> The first synthesis of a Type II alkaloid (himandridine) was recently reported by Movassaghi.<sup>9</sup> Additional approaches to the syntheses of Type III alkaloids have also been reported by Sarpong<sup>7d</sup> and Ma.<sup>7e</sup>

In this article, we provide a full account of our synthesis of *ent*-galbulimima alkaloid GB 13 and *ent*-himgaline (Scheme 1).<sup>10</sup> We also provide new experimental and computational insights regarding the pivotal imine aldol addition step gained during our current efforts directed toward the Type II alkaloid himandridine. Notably, the desired aldol process was found to be spontaneous in protic solvents, conditions congruent with the proposed biosynthesis of these alkaloids. Computational modeling of the thermochemistry of these and related imine aldol additions indicates that these additions are nearly thermoneutral.

Subsequent analysis of the GB alkaloid polycycle reveals an unexpected conformational preference that suggests a steric rationale for why certain imine substrates readily cyclize while others are unreactive.

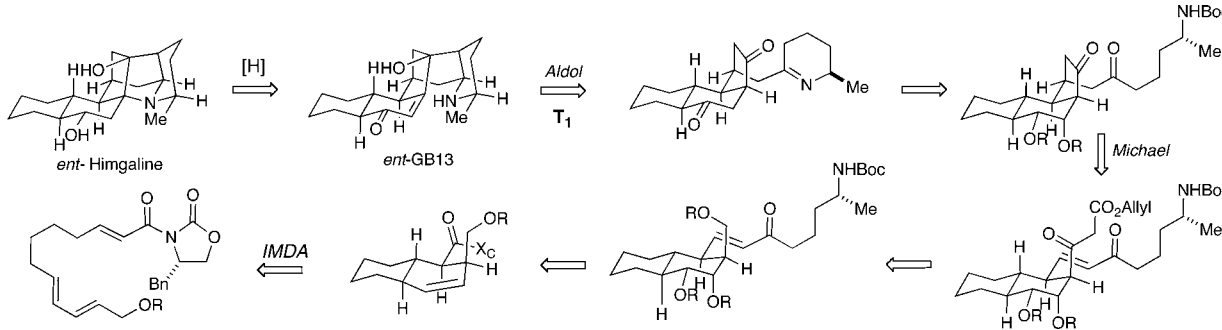
## TYPE III ALKALOIDS

**Synthesis Plan.** Our strategy for the synthesis of the GB alkaloids was influenced by the Ritchie/Taylor<sup>11</sup> biosynthetic hypothesis that has subsequently been elaborated by others.<sup>11</sup> In this proposal, a monocyclic polyketide precursor undergoes a succession of intramolecular bond constructions: Diels–Alder

Received: January 6, 2012

Published: April 25, 2012

Scheme 1. Proposed Synthesis Plan for Type III GB Alkaloids



cycloaddition, Michael, and imine aldol addition to construct the polycyclic skeleton shared by the Type II and Type III alkaloids. The current plan has integrated each of these bond constructions (Scheme 1). With respect to the Type III alkaloids, we anticipated that himgaline might arise from GB 13 after *N*-conjugate addition and stereoselective reduction at C16. The bicyclo[3.2.1]octane himgaline core was envisioned to arise from a keto-imine, which might undergo an imine aldol addition, and iminium ion reduction to provide the desired polycyclic skeleton. An intramolecular Michael addition was envisioned to construct the necessary cyclopentanone moiety. The Michael precursor might then be derived from the elaboration of an appropriately functionalized decalin, which could be obtained in enantiopure form via auxiliary-controlled intramolecular Diels–Alder (IMDA) cycloaddition.

## RESULTS AND DISCUSSION

**Synthesis of ent-GB 13 and ent-Himgaline.** Synthesis of *ent*-himgaline began with 6,6-dimethoxyhexanal (**1**)<sup>12</sup> which underwent a vinylogous Horner–Wadsworth–Emmons (HWE) olefination with triethyl 4-phosphonocrotonate (Scheme 2). Following ester reduction and alcohol protection,

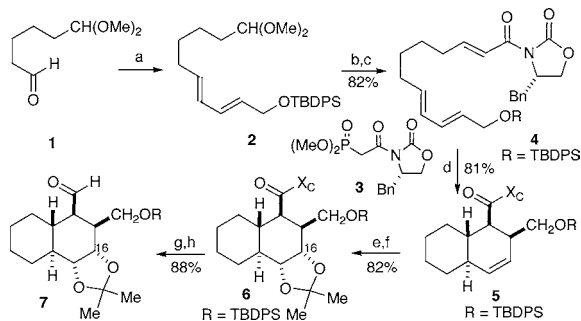
of the chiral auxiliary to provide the derived thioester was followed by semireduction to provide aldehyde **7**.

Olefination of **7** with phosphonate **8<sup>sd</sup>** afforded the desired enone for the anticipated intramolecular Michael addition (Scheme 3). Efforts to desilylate **9** in preparation for introduction of the needed  $\beta$ -ketoester were complicated by irreversible *O*-conjugate addition to provide tetrahydrofuran **10**. A single product diastereomer was produced, with the configuration at the newly formed stereocenter matching that desired for the planned intramolecular Michael addition (NOE analysis). Nonselective ketone reduction of **9** followed by silyl deprotection provided diol **11** while avoiding the undesired conjugate addition process. *N*-Benzylation<sup>15</sup> to provide **12** was followed by simultaneous oxidation of both alcohols with Dess–Martin periodinane.<sup>16</sup>

A Roskamp reaction with allyl diazoacetate<sup>17</sup> and the keto-aldehyde derived from **12** incorporated the necessary  $\beta$ -ketoester that, after purification or storage at  $-20\text{ }^{\circ}\text{C}$ , was obtained primarily as **13**, the product of  $\beta$ -ketoester enol addition. As anticipated, enol addition proved to be reversible under basic conditions: a combination of lithium methoxide and lithium perchlorate in ether, conditions reported to provide chelated  $\beta$ -ketoester anions,<sup>18</sup> provided the desired Michael adduct **14** in 62% yield over the three steps.

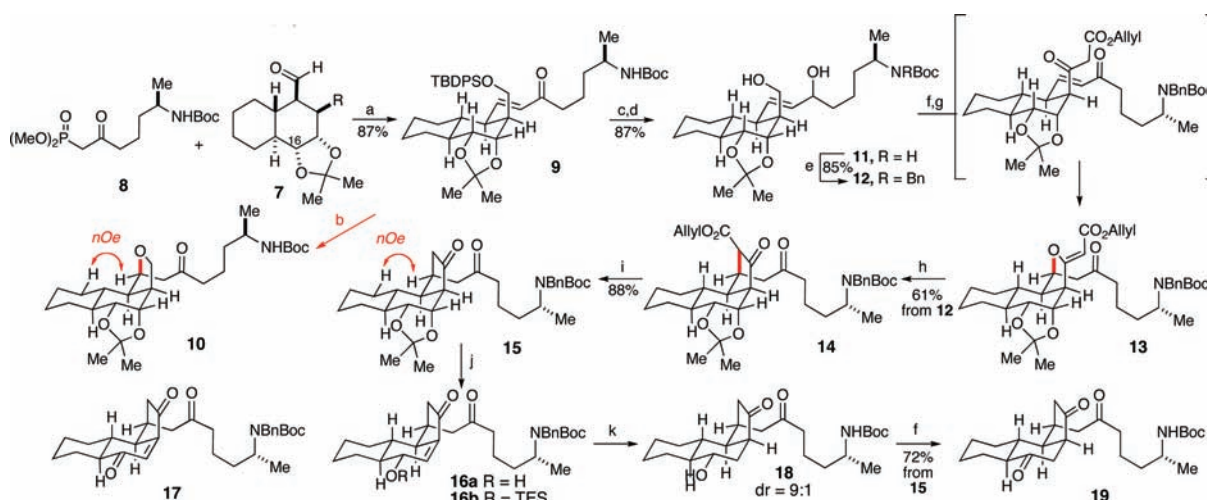
The diastereoselectivity of this process could not be directly assessed due to the carboalkoxy substituent; however, palladium-catalyzed decarboxylation of the allyl ester resulted in the isolation of a single cyclopentanone diastereomer **15**, leading to the conclusion that the Michael addition had proceeded with high selectivity. Most likely a favored extended conformation of the enone acceptor explains the observed outcome. However, when the Michael addition was promoted by cesium carbonate in ethanol, the stereoselectivity eroded (3:1). Such conditions are reported to provide dipole minimized  $\beta$ -ketoester enolates,<sup>18</sup> suggesting that the  $\beta$ -ketoester enolate geometry may play a secondary role in determining the diastereoselectivity in this Michael addition.

Although our synthesis plan called for an imine/enamine aldol addition, it is also evident that an enolate aldol addition followed by amine deprotection and condensation might also be considered in the construction of the requisite bicyclo[3.2.1]octane synthon (Scheme 4).<sup>19</sup> Unfortunately, under a variety of enolization conditions across a variety of substrates, no enolate aldol addition products were observed with substrates related to either **16b** or **18** (Scheme 3). The overriding reactivity of the cyclopentanone moiety toward enolization proved to be the obstacle in all instances.<sup>20</sup> These results reinforced the commitment to the intramolecular enamine aldol approach.

Scheme 2. Synthesis of Functionalized Decalin Subunit<sup>a</sup>

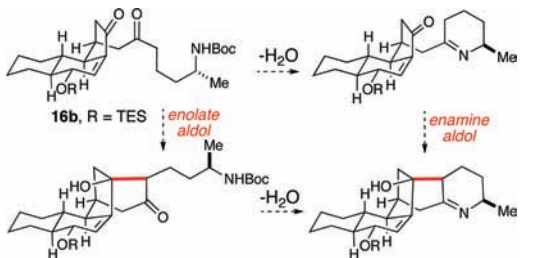
<sup>a</sup>Conditions: (a) See Supporting Information; (b) LiBF<sub>4</sub>, MeCN, H<sub>2</sub>O; (c) 3, LiCl, *i*-Pr<sub>2</sub>NEt, MeCN; (d) Me<sub>2</sub>AlCl, PhMe,  $-30\text{ }^{\circ}\text{C}$ ; (e) K<sub>2</sub>O<sub>s</sub>O<sub>4</sub>, NMO, acetone/pH 7 buffer; (f) dimethoxyp propane, TsOH, acetone; (g) LiSEt, THF, 0 °C; (h) DIBAL-H, PhMe,  $-90\text{ }^{\circ}\text{C}$ .

acetal **2** was cleaved to the derived aldehyde. A second HWE olefination with phosphonate **3** then incorporated the illustrated chiral auxiliary.<sup>13</sup> The desired IMDA cycloaddition was effected using Me<sub>2</sub>AlCl to provide decalin **5** in 81% yield as a single diastereomer.<sup>14</sup> The necessary oxygenation at C16 was incorporated by a diastereoselective dihydroxylation, which was followed by diol protection as its derived acetonide **6**. Removal

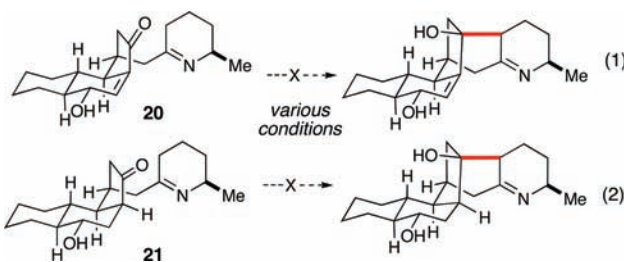
Scheme 3. Intramolecular Conjugate Additions and Elaboration to Substrates for Aldol Cyclization<sup>a</sup>

<sup>a</sup>Conditions: (a) *i*-Pr<sub>2</sub>NEt, LiCl, MeCN; (b) TBAF, HOAc, THF; (c) DIBAL, PhMe, -90 °C; (d) TBAF, HOAc, THF; (e) see Supporting Information; (f) DMP, NaHCO<sub>3</sub>, CH<sub>2</sub>Cl<sub>2</sub>; (g) allyldiazoacetate, SnCl<sub>2</sub>; (h) LiOMe, LiClO<sub>4</sub>, Et<sub>2</sub>O, 0–23 °C; (i) Pd(PPh<sub>3</sub>)<sub>4</sub>, morpholine, THF; (j) DBU, PhH; (k) Pd(OH)<sub>2</sub>, H<sub>2</sub>, THF.

Scheme 4. Complementary Aldol Constructors



**Ent-Himgaline and Ent-GB 13.** Scheme 3 summarizes the construction of advanced intermediates for both the himgaline and GB 13 syntheses. Several opportunities for the implementation of the imine aldol construction are possible from these intermediates. These options were then evaluated. We were unable to effect aldol addition with imine 17. In another study, imine 20 was subjected to a broad survey of reaction conditions; however, no evidence for the desired aldol addition was obtained (eq 1). Again, 21 also proved resistant to aldol addition (eq 2). These cases illustrate the tenuous nature of the aldol addition process.

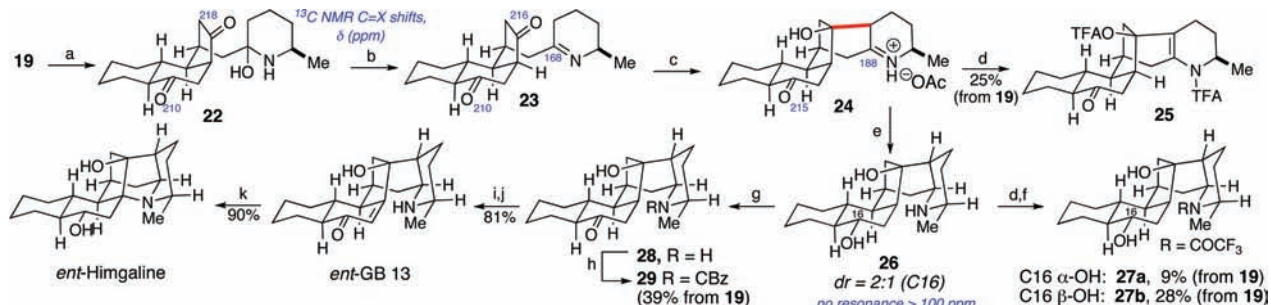


Triketone 19 (Scheme 3) ultimately proved to be a tractable substrate for the requisite aldol transformation (Scheme 5). Carbamate deprotection and dehydration of the resulting hemiaminal 22 afforded imine 23, which gratifyingly provided the desired aldol adduct 24 upon treatment with acetic acid in THF (Scheme 5). *In situ* <sup>13</sup>C NMR spectroscopy proved especially useful during this sequence of transformations, as

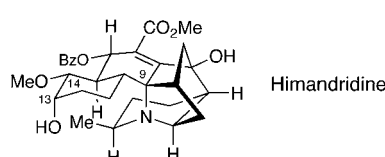
changes to the C=O and C=N resonances (160–220 ppm) provided clear indications of reaction progress at each stage. Acylation of iminium ion 24 with TFAA provided enamide 25 as the principal product, confirming successful aldolization. As 25 proved resistant to a variety of transition metal catalyzed and ionic hydrogenation conditions, reduction of the iminium ion prior to acylation was pursued. Sodium cyanoborohydride was chosen to minimize unwanted reduction of the cyclohexanone moiety; however, under all conditions investigated both the iminium ion and cyclohexanone were reduced to provide amino alcohol 26. Although full diastereocontrol was observed at the three stereocenters formed during the aldol addition and iminium ion reduction, the ketone reduction proceeded to give a 2:1 mixture of axial and equatorial alcohol epimers. Initially, this mixture was peracylated with TFAA to provide chromatographically tractable material. Saponification of the trifluoroacetates provided separable diols 27a and 27b; as 27a spectroscopically matched an intermediate encountered during Mander's synthesis of GB 13, a formal total synthesis of GB 13 had been completed.

In subsequent iterations, the mixture of C16 alcohol epimers 26 was reoxidized using DMP immediately following iminium ion reduction. The high chemoselectivity observed in this oxidation is likely derived from the highly hindered environment surrounding the secondary amine. Acylation of keto-amine 28 using benzyl chloroformate facilitated purification of carbamate 29, which was isolated in 39% yield over six steps. No unwanted diastereomers were isolated from this process. The necessary unsaturation was introduced using IBX<sup>7b</sup> (90%); TMSI then cleaved the benzyl carbamate to deliver *ent*-GB 13.<sup>7b</sup> Synthetic GB 13 matched a natural sample spectroscopically and gave an optical rotation of similar magnitude but opposite sign (*ent*-GB 13,  $[\alpha]^{20}_D +71.6$  (*c* 0.2, CHCl<sub>3</sub>); GB 13,  $[\alpha]^{20}_D -76$  (*c* 1.0, CHCl<sub>3</sub>)).

The conversion of (+)-GB 13 to (+)-himgaline required conjugate addition of the piperidine nitrogen to the pendant enone and stereoselective reduction of the C16 ketone. During isolation and purification of GB 13, it became clear that even trace quantities of acid promoted the desired N-conjugate addition to an appreciable extent (10–15%). Stirring (+)-GB

Scheme 5. Ent-GB 13 and Ent-Himgaline Syntheses<sup>a</sup>

13 in a 1:1 mixture of acetic acid and acetonitrile fully promoted the desired conjugate addition within minutes;<sup>22</sup> subsequent addition of sodium triacetoxyborohydride initiated directed hydride delivery to furnish *ent*-himgaline in 90% yield. Synthetic himgaline was spectroscopically identical to a natural sample and gave an optical rotation of similar magnitude but opposite sign (*ent*-himgaline,  $[\alpha]^{20}_D +80.0$  (*c* 0.1, CHCl<sub>3</sub>); himgaline,  $[\alpha]^{20}_D -84$  (*c* 1.0, CHCl<sub>3</sub>)).

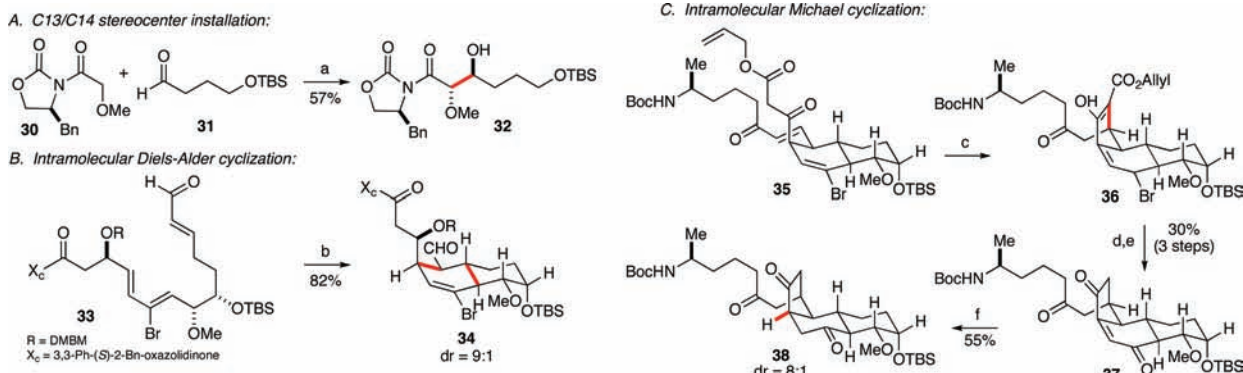


**Progress toward the Synthesis of Himandridine.** We next sought to extend our previously disclosed synthesis of himgaline to the type II alkaloid himandridine, which features additional oxygenated stereocenters at C13 and C14 as well as attachment of nitrogen at C9 rather than C19 (Figure 1). Although our synthesis plan remained similar to our himgaline approach (Scheme 1), the structure of himandridine ultimately required that each of our key intramolecular cyclization steps be revised. To address the addition of oxygenation at C13 and C14, we relied on previously developed Sn(II)-promoted antiselective glycolate aldol methodology (Scheme 6).<sup>23</sup> Good diastereoselectivity was observed in this process (3 to 1, desired to sum of undesired isomers), and the desired adduct was

isolated in 57% yield. Elaboration of this synthon using standard conditions allowed assembly of polyene 33, a substrate for cycloaddition. In contrast to our himgaline approach (Scheme 2), diastereoselectivity was predicted to be controlled by 1,3-allylic strain at C14.<sup>24</sup> Gratifyingly, under thermal activation polyene 34 cyclized to the desired Diels–Alder adduct in high yield and diastereoselection (82%, 9:1 dr). Subsequent installation of the enone Michael acceptor and  $\beta$ -keto ester led to 35, a substrate for the planned intramolecular Michael cyclization. Under conditions established during the synthesis of himgaline (LiClO<sub>4</sub>, LiOMe, Et<sub>2</sub>O; Scheme 3), Michael addition was accompanied by olefin isomerization to allylic bromide 36. Use of milder soft enolization conditions (LiBr, NEt<sub>3</sub>, EtOAc) suppressed formation of side products but did not prevent olefin migration. The unstable C16 allylic bromide subsequently underwent oxidation to the derived ketone in the presence of silver(I) trifluoroacetate and air.<sup>25</sup> Allyl ester removal and stereoselective olefin reduction (Zn, HOAc) led to triketone 38, a substrate for imine aldol cyclization in analogy to our himgaline precedent (Scheme 5).

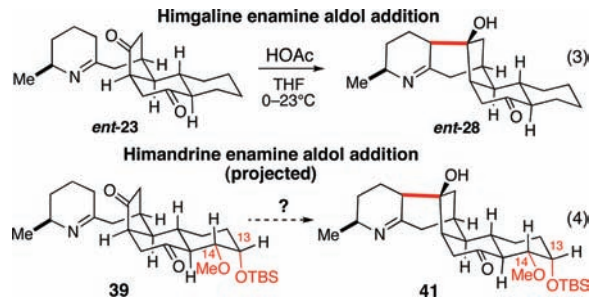
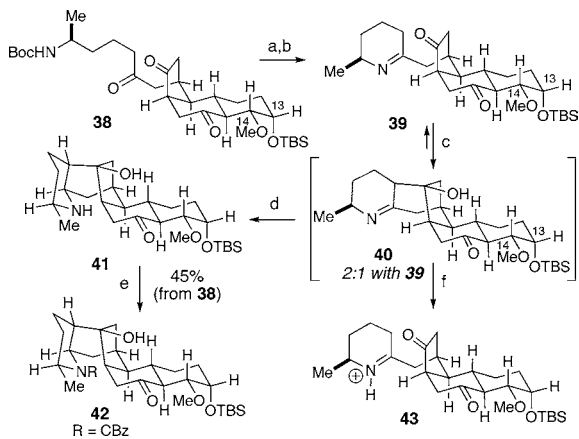
**Imine Aldol Additions: Himandridine.** The synthesis plan for himandridine was based on the himgaline precedent for the analogous aldol construction (Scheme 7).

The synthesis of imine 39 is outlined in Scheme 8. Surprisingly, this substrate did not undergo the anticipated aldol addition under conditions identical to those used during the himgaline synthesis (eq 3 vs eq 4). These observations prompted a study of solvent effects on the aldol process. After

Scheme 6. Key Steps toward the Synthesis of Himandridine<sup>a</sup>

<sup>a</sup>Conditions: (a) Sn(OTf)<sub>2</sub>, NEt<sub>3</sub>, TMEDA, CH<sub>2</sub>Cl<sub>2</sub>, –78 °C; (b) PhMe, BHT, reflux, 48 h; (c) LiBr, iPr<sub>2</sub>NEt, EtOAc, 0 °C; (d) Ag(I) trifluoroacetate, DMF, air; (e) Pd(PPh<sub>3</sub>)<sub>4</sub>, morpholine, THF; (f) Zn, HOAc.

## Scheme 7. Comparative Enamine Aldol Additions

Scheme 8. Enamine Aldol Addition Directed toward Himandridine<sup>a</sup>

<sup>a</sup>Conditions: (a) TFA, CH<sub>2</sub>Cl<sub>2</sub>; (b) 4 Å mol. sieves, PhH; (c) MeOH, 45 min; (d) same pot: HOAc, NaBH<sub>3</sub>CN, 0 °C; (e) benzyl chloroformate, Na<sub>2</sub>CO<sub>3</sub>, H<sub>2</sub>O, CH<sub>2</sub>Cl<sub>2</sub>; (f) remove MeOH; add CDCl<sub>3</sub>, 16 h.

further investigation, it was found that the dissolution of 39 in methanol was sufficient to induce formation of the desired aldol adduct as a ca. 2:1 mixture with starting material (Scheme 8, Table 1). In further contrast to our experience during the himgaline synthesis, reduction of the resultant iminium ion with

Table 1. Solvent Dependence on Aldol Addition

39  $\xrightarrow[\text{solvent, } 30 \text{ min}]{\text{NaBH}_4, \text{HOAc}}$  41 + 44

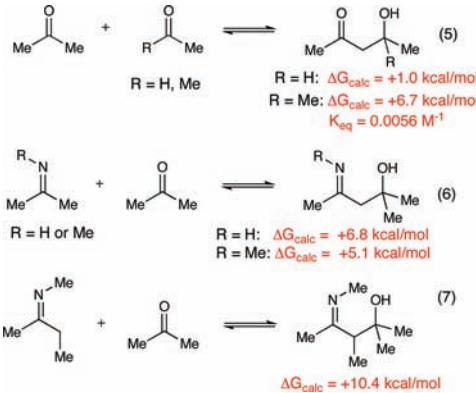
solvent	41 <sup>a</sup>	44
CH <sub>3</sub> OH	67	33
CD <sub>3</sub> OD + 1% NEt <sub>3</sub> <sup>b</sup>	67	33
CD <sub>3</sub> OD + 1% HOAc <sup>b</sup>	67	33
i-PrOH	55	45
CF <sub>3</sub> CH <sub>2</sub> OH <sup>c</sup>	40	60
HOCH <sub>2</sub> CH <sub>2</sub> OH	33	67
1:1 formamide/MeCN	20	80
1:1 water/MeCN	0	100
1:1 water/MeOH	33	67

<sup>a</sup>Ratio of 41 to 44 estimated from <sup>1</sup>H NMR spectra. <sup>b</sup>Substantial incorporation of deuterium was observed. <sup>c</sup>Unidentified byproducts observed.

sodium cyanoborohydride spared the C16 ketone; following N-acylation, the desired polycyclic adduct 42 (Scheme 8) was obtained in 45% yield over four steps.<sup>26</sup> As before, no unwanted diastereomers were obtained from this sequence.

When aldol cyclization of 39 was monitored by <sup>1</sup>H NMR spectroscopy (*d*<sub>4</sub>-MeOH), maximal product formation was achieved within 45 min of dissolution. Neither prolonged reaction times (24 h) nor addition of acetic acid or triethylamine to the reaction mixture altered the product distribution. As cyclization of 39 was spontaneous in methanol but not in chloroform, benzene, or THF, a methanol solution of aldol adduct 40 was concentrated to dryness and redissolved in CDCl<sub>3</sub>. Over a period of 16 h, complete retro-aldolization was observed with apparent concomitant formation of iminium ion 43.<sup>27</sup> This result confirmed the previously observed lack of reactivity in aprotic solvents, even under acidic conditions. *This highlights the fact that both aldol addition and retro-aldolization in this system can be dynamic processes.* Table 1 highlights the effectiveness of a variety of protic media in the aldolization with methanol being the solvent of choice.

**Computations: Aldol Addition Thermochemistry.** As the factors determining enamine aldol reactivity in these systems were not apparent, a computational study was undertaken to elucidate reaction energetics and conformational preferences of reactants, transition states, plausible intermediates, and products. Since our experimental data document that these reactions can be reversible at room temperature, we first focused on the overall thermodynamics of these imine aldol additions in comparison with their aldol counterparts (eqs 5–7).

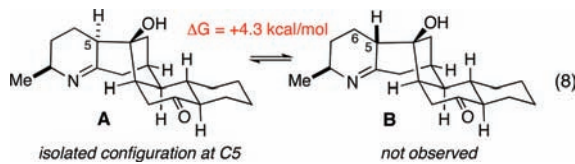


The energetics of aldolization can be viewed as a nearly balanced competition between a favorable reaction enthalpy and the unfavorable entropy inherent to bimolecular reactions (*ca.* 12 kcal/mol).<sup>28</sup> For example, aldol dimerization of acetone to provide diacetone alcohol is minimal at equilibrium,<sup>29,30</sup> while aldehyde electrophiles are computed to be substantially more favorable (eq 5).<sup>31</sup> Analogous calculations predict the aldol addition of simple acetone-derived imines to acetone to be disfavored by 5–7 kcal/mol (eq 6), similar to the dimerization of acetone. When imine geometry precludes hydrogen bonding between the product imine and tertiary hydroxyl, as in the GB alkaloid cases, the reaction is additionally disfavored (eq 7). Imine aldol additions to ketones are thus likely to be thermodynamically favorable only in an intramolecular setting where the entropic penalty for reaction is significantly diminished.

To determine whether the imine aldol reactions encountered in our synthesis studies are consistent with thermodynamic

control, we employed conformational searching and density functional theory methods to identify the global conformational minimum for each imine reactant and product (M06-2X/6-31 g(d); see Supporting Information).<sup>32,33</sup> SMD continuum solvent modeling allowed investigation of the role of solvent effects as noted experimentally.<sup>31b</sup>

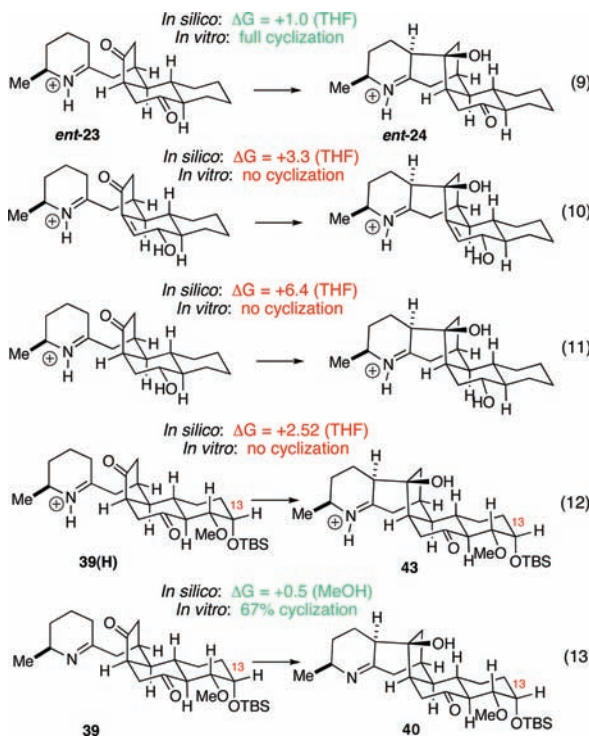
An initial stereochemical issue addressed in this analysis involves the two possible C5 aldol product diastereomers (**A**, **B**) that may be formed through addition from either enamine diastereoface (eq 8). It is presumed that these diastereomers



might be readily interconvertible through imine-enamine tautomerism. Both product structures were modeled. In each case, the naturally occurring C5 isomer **A** was found to be 3.7–4.9 kcal/mol more favorable than its epimer **B**, consistent with our isolation of only the naturally occurring diastereomer **A**. Formation of epimer **B** substantially alters the bicyclo[3.2.1]-octane conformation and places the C6 and hydroxyl substituents in an eclipsing orientation, which may explain the computed energy difference (eq 8 and Supporting Information).

The computed reaction energies for these additions correlate with the experimental data (Scheme 9). Although the reaction free energies appear to be generally overestimated, successful reactions are substantially more favorable than those that resist cyclization. For example, in THF, the aldolization carried out in the synthesis of himgaline (23–24) is predicted to be energetically disfavored by  $\Delta G = +1.0$  kcal/mol (Scheme 9,

#### Scheme 9. Computational and Experimental Results



eq 9). By contrast, cyclizations of iminium ions that did not undergo aldol addition under identical conditions are predicted to be energetically more costly by  $\Delta\Delta G = +1.5$ –5.4 kcal/mol (eqs 10–12). Additionally, cyclization of imine **39** is predicted to be 2 kcal/mol more energetically favorable in methanol than in THF using our standard conditions. This outcome is consistent with the observed cyclization of this substrate in MeOH (eq 13) but not THF (eq 12) or other aprotic solvents. Since the implicit solvation methods used do not account for H-bonding effects, other parameters, including the smaller molecular product surface area, are likely responsible for the altered energetics. *In summary, these imine aldol additions may be run under neutral conditions as long as H-bonding solvents such as methanol are employed.*

The computational findings also correlate well with experimental results when applied to substrates reported by Movassaghi to undergo analogous enamine aldol additions,<sup>34</sup> including those encountered in their total syntheses of the GB alkaloids GB 13<sup>7b</sup> and himandrine (see Supporting Information).<sup>9</sup> As their conditions are ambiguous as to whether the important aldol addition takes place immediately following an initial cuprate addition in THF or during a subsequent reaction in ethanol/water, both THF and ethanol were modeled (implicit solvation). Once again, the reactions are predicted to be more favorable (by 1.7–2.8 kcal/mol) in ethanol than THF. Calculated reaction energies in ethanol range from −0.8 kcal/mol to +1.2 kcal/mol, similar to our successful cases and substantially lower than our unsuccessful cases. The trends in computed energies of reaction thus correctly predict the observed reactivities across all cases modeled, with the five successful reactions shown to be on average 3.9 kcal/mol more energetically favorable than the three cases in which cyclization was not observed.

As the origin of the energy differences across our reactions remained unclear, we next undertook an analysis of the energy-minimized conformations of each of our reactants and products. Although the lowest-energy conformers of the starting materials are nearly identical and feature the expected chair–chair conformation in the decalin ring system, the low energy conformers of the bicyclo[3.2.1]octane products uniformly display a B ring boat conformation (Figure 3). This conformational preference was also observed for all-carbon tricyclic ring system **45**, in which a B ring boat conformation was computed (M06-2X/6-31 g(d)) to be energetically favored over the nearest conformer (an approximate chair) by 3.7 kcal/mol (Figure 2). Likewise, a search of the Cambridge Crystallographic Database revealed two highly analogous ring systems in which the cis-fused cyclohexane also adopts a boat geometry.<sup>35</sup> These examples include an intermediate accessed during Mander's synthesis of

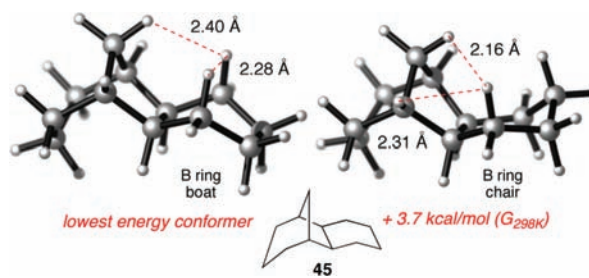


Figure 2. Computed conformations of an alkane ring system.

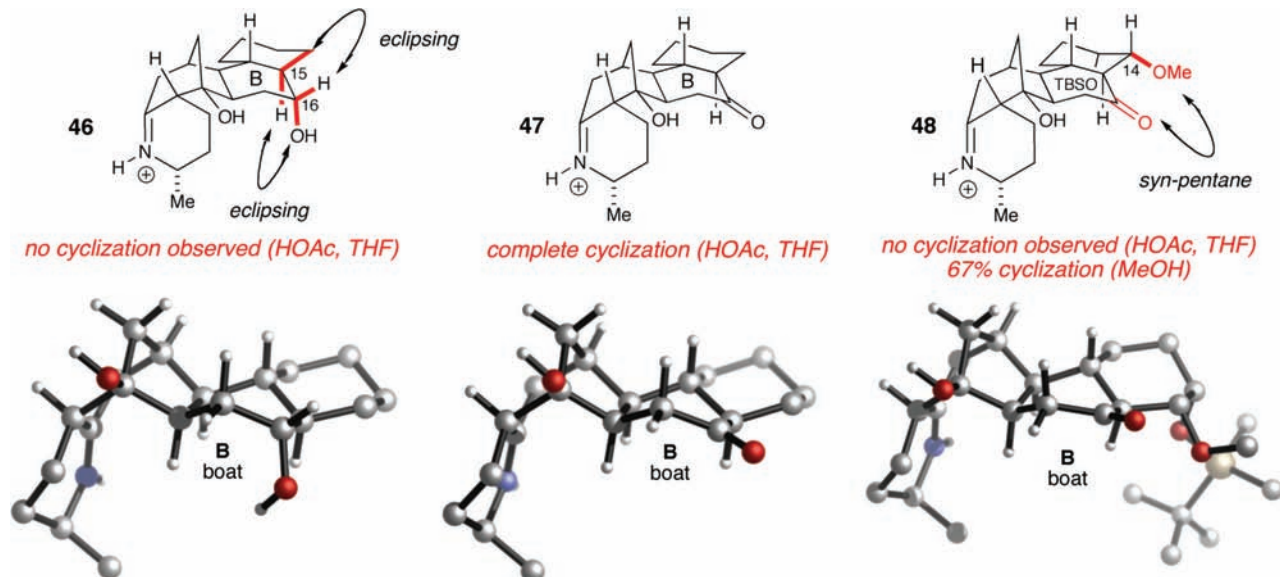


Figure 3. Energy minimized enamine aldol addition products.

GB 13,<sup>7</sup> highlighting the ability of our computational approach to capture known features of the GB ring system. Taken together, these data suggest the unanticipated preference for the B ring boat conformation is dictated by the conformational constraints of the rigid bicyclo[3.2.1]octane system. The boat conformation also appears to maximize interatomic distances between hydrogen atoms that are within van der Waals contact or nearly so (Figure 2).

This counterintuitive product conformation may provide a rationale for the experimentally observed patterns of reactivity based on product stability if the reactions are reversible under the experimental conditions (as was observed for 39/40). Aldol adduct 46, which was never obtained, would encounter unfavorable eclipsing interactions at C15 and C16 as a result of the favored product boat conformation (Figure 3). By contrast, aldol adduct 47, which formed readily in HOAc/THF, instead accommodates the ketone carbonyl in a more favorable bisected conformation.

Additional oxygenation at C13 and C14, as required for himandridine, gives rise to aldol adduct 48, which did not form in HOAc/THF but did proceed to *ca.* 67% conversion in methanol. Due to the favored product boat conformation, the C14 substituent creates a destabilizing *syn*-pentane-type interaction with the C16 carbonyl oxygen that likely impedes the desired cyclization (Figure 3). The energy-minimized structure of 48 deviates noticeably from an ideal boat geometry, likely to mitigate the impact of this destabilizing interaction.

**Computations: Enamine Aldol Transition States.** To complement the above thermodynamic analysis, we next sought to identify transition states and plausible intermediates en route to the observed cyclized enamine aldol products. Although transition states for enamine aldol additions, including an intramolecular cyclization, have been studied,<sup>36</sup> the GB alkaloid case differs from previously analyzed systems. Specifically, the geometric constraints of the forming bicyclo[3.2.1]octane ring system preclude the closed transition states known to be favorable in less restricted imine aldol reactions. Therefore, we modeled the geometrically feasible open transition state orientations under both sets of conditions shown to be capable

of promoting the desired cyclization, dissolution in methanol and stoichiometric acetic acid in THF.

Computations indicate the reaction takes a very different course in methanol than in tetrahydrofuran. In methanol, the lowest energy transition state obtained for the formation of 40 (Scheme 7) was zwitterion-like and late, with a forming bond length of 1.97 Å (Figure 4, 48-TS). The computed activation

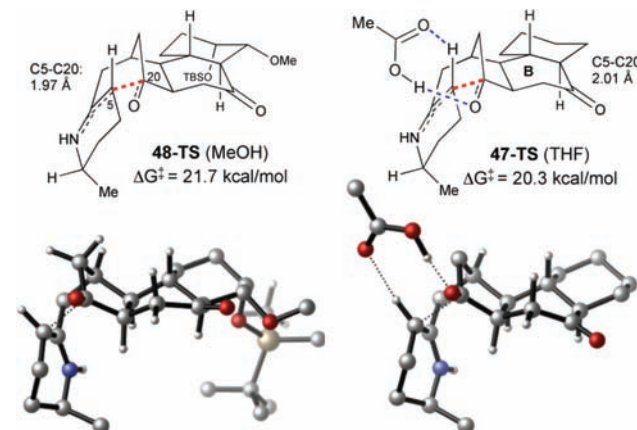


Figure 4. Computed transition states.

energy, 21.7 kcal/mol, together with our computed free energy of reaction (+0.5 kcal/mol) is consistent with our experimental observation of a facile but incomplete reaction at room temperature.<sup>37</sup> Additionally, as previously observed,<sup>36</sup> a zwitterion intermediate was also located at an energy of +17.1 kcal/mol. Both the lowest-energy transition state and zwitterion intermediate displayed a B-ring boat conformation (Figure 4), indicating the importance of this conformational change during bond formation as well as in the ground state (Figure 3). Transition states possessing a half-chair B-ring conformation were higher in energy by at least 0.9 kcal/mol.<sup>37</sup> By contrast, in THF, neither an analogous transition state nor a zwitterion intermediate could be located. Structures with the newly formed aldol bond length constrained to 1.67 Å, a typical distance for zwitterion intermediates in methanol, were severely

disfavored relative to the methanol case ( $\Delta\Delta E$  ca. 19 kcal/mol). The role of methanol (but not nonpolar solvents) in promoting the spontaneous formation of **40** thus appears two-fold: in addition to lowering the free energy of reaction relative to nonpolar solvents, methanol also provides substantial stabilization to zwitterion-like transition states, enabling bond formation to occur at room temperature.

We next examined transition states in THF with an explicit acetic acid molecule, mirroring conditions used in the successful cyclization to provide **47**. Multiple orientations of the acetic acid molecule were examined, with two modes giving rise to transition states of reasonable energy (see Supporting Information). In the first ( $\Delta G^\ddagger = +22.2$  kcal/mol), acetic acid serves as a hydrogen bond donor to the cyclopentanone oxygen during bond formation, providing superior delocalization of the forming anion relative to THF alone. In the second and lowest-energy transition state ( $\Delta G^\ddagger = +20.3$  kcal/mol), acetic acid both donates a hydrogen bond to the cyclopentanone oxygen and accepts a hydrogen bond from the vinylic proton on the reacting enamine carbon (Figure 4, **47-TS**).

## CONCLUSIONS

The proposed strategy of sequential intramolecular Diels–Alder, Michael, and imine aldol cyclizations to construct the complex architectures of the GB alkaloids has delivered total syntheses of GB 13 and himgaline as well as an advanced intermediate directed toward the type II alkaloid himandridine. The pivotal imine aldol addition common to these syntheses was found to be highly sensitive to subtle changes in both substrate structure and reaction conditions. Although kinetic control in these cyclizations cannot be rigorously excluded, the observation of reversibility in one case together with computational predictions of near-thermoneutrality and accessible activation energies lead us to favor a model in which these reactions are under thermodynamic control. Calculated free energies of reaction correlate well with observed reactivity, and energy-minimized structures predict an unexpected boat cyclohexane conformation previously observed by X-ray crystallographic analysis of a closely related structure. Further conformational analysis suggests a rationale for the observed reactivity in which the aldol products of unsuccessful substrates, but not successful substrates, face destabilizing steric interactions as a direct result of the strong bias for a B-ring boat conformation. At present, two strategies to facilitate the production of the desired aldol product have been demonstrated: incorporation of  $sp^2$  hybridization at C16 and the use of a protic solvent. Interestingly, both manipulations likely bring our system closer to the environment of the biosynthesis of these alkaloids. These studies highlight the unexpected complexities of natural products synthesis and the power of computational methods to provide insight into challenging reactivities.

## ASSOCIATED CONTENT

### Supporting Information

Experimental procedures, compound characterization data, and computational details. This information is available free of charge via the Internet at <http://pubs.acs.org>.

## AUTHOR INFORMATION

### Corresponding Author

evans@chemistry.harvard.edu

## Notes

The authors declare no competing financial interest.

## ACKNOWLEDGMENTS

We thank Prof. Lewis N. Mander for generous donations of naturally isolated GB 13 and himgaline. This work was supported by the National Institutes of Health (GM-33328-20) and Amgen.

## REFERENCES

- (a) Ritchie, E.; Taylor, W. C. In *The Alkaloids*; Manske, R. H. F., Ed.; Academic Press: New York, 1967; Vol. 9, Chapter 14, p 529.
- (b) Collins, D. J.; Culvenor, C. C. J.; Lamberton, J. A.; Loder, J. W.; Price, J. R. *Plants for Medicines. A Chemical and Pharmacological Survey of Plants in the Australian Region*; CSIRO: Melbourne, 1990; Chapter 1.
- (c) Pinhey, J. T.; Ritchie, E.; Taylor, W. C. *J. Aust. Chem.* **1961**, *14*, 106–126.
- (d) Binns, S. V.; Dunstan, P. J.; Guise, G. B.; Holder, G. M.; Hollis, A. F.; McCredie, R. S.; Pinhey, J. T.; Prager, R. H.; Rasmussen, M.; Ritchie, E.; Taylor, W. C. *J. Aust. Chem.* **1965**, *18*, 569–573.
- (e) Mander, L. N.; Ritchie, E.; Taylor, W. C. *J. Aust. Chem.* **1967**, *20*, 981–1019.
- (f) Mander, L. N.; Ritchie, E.; Taylor, W. C. *J. Aust. Chem.* **1967**, *20*, 1021–1027.
- (g) Guise, G. B.; Mander, L. N.; Prager, R. H.; Rasmussen, M.; Ritchie, E.; Taylor, W. C. *J. Aust. Chem.* **1967**, *20*, 1029–1035.
- (h) Mander, L. N.; Prager, R. H.; Rasmussen, M.; Ritchie, E.; Taylor, W. C. *J. Aust. Chem.* **1967**, *20*, 1473–1491.
- (i) Mander, L. N.; Prager, R. H.; Rasmussen, M.; Ritchie, E.; Taylor, W. C. *J. Aust. Chem.* **1967**, *20*, 1705–1718.
- (2) Thomas, B. *Eleusis: J. Psychoact. Plants Compd.* **1999**, *3*, 82–90.
- (3) (a) Kozikowski, A. P.; Fauq, A. H.; Miller, J. H.; McKinney, M. *Bioorg. Med. Chem. Lett.* **1992**, *2*, 797–802. (b) Malaska, M. J.; Fauq, A. H.; Kozikowski, A. P.; Aagaard, P. J.; McKinney, M. *Bioorg. Med. Chem. Lett.* **1995**, *5*, 61–66.
- (4) (a) Clasby, M. C.; Chackalamannil, S.; Czarniecki, M.; Doller, D.; Eagen, K.; Greenlee, W. J.; Lin, Y.; Tsai, H.; Xia, Y.; Ahn, H.-S.; Agans-Fantuzzi, J.; Boykow, G.; Chintala, M.; Foster, C.; Bryant, M.; Lau, J. *Bioorg. Med. Chem. Lett.* **2006**, *16*, 1544–1548. (b) Chackalamannil, S.; Xia, Y. *Expert Opin. Ther. Pat.* **2006**, *16*, 493–505. (c) Chackalamannil, S.; Wang, Y.; Greenlee, W. J.; Hu, Z.; Xia, Y.; Ahn, H.-S.; Boykow, G.; Hsieh, Y.; Palomanda, J.; Agans-Fantuzzi, J.; Kurowski, S.; Graziano, M.; Chintala, M. *J. Med. Chem.* **2008**, *51*, 3061–3064.
- (5) (a) Hart, D. J.; Wu, W.-L.; Kozikowski, A. P. *J. Am. Chem. Soc.* **1995**, *117*, 9369–9370. (b) Chackalamannil, S.; Davies, R. J.; Aserom, T.; Doller, D.; Leone, D. *J. Am. Chem. Soc.* **1996**, *118*, 9212–9213.
- (c) Takadoi, M.; Katoh, T.; Ishiwata, A.; Terashima, S. *Tetrahedron Lett.* **1999**, *40*, 3399–3402.
- (d) Tchabanenko, K.; Adlington, R. M.; Cowley, A. R.; Baldwin, J. E. *Org. Lett.* **2005**, *7*, 585–588.
- (e) Tchabanenko, K.; Chesworth, R.; Parker, J. S.; Anand, N. K.; Russell, A. T.; Adlington, R. M.; Baldwin, J. E. *Tetrahedron* **2005**, *61*, 11649–11656.
- (6) (a) Chackalamannil, S.; Doller, D.; McQuade, R.; Ruperto, V. *Bioorg. Med. Chem. Lett.* **2004**, *14*, 3967–3970. (b) Doller, D.; Chackalamannil, S.; Czarniecki, M.; McQuade, R.; Ruperto, V. *Bioorg. Med. Chem. Lett.* **1999**, *9*, 901–906. (c) Takadoi, M.; Katoh, T.; Ishiwata, A.; Terashima, S. *Tetrahedron* **2002**, *58*, 9903–9923.
- (7) (a) Mander, L. N.; McLachlan, M. M. *J. Am. Chem. Soc.* **2003**, *125*, 2400–2401. (f) McLachlan, M. M. Ph.D. thesis, Research School of Chemistry, Australian National University, 2002. (b) Movassagh, M.; Hunt, D. K.; Tjandra, M. *J. Am. Chem. Soc.* **2006**, *128*, 8126–8127.
- (c) Shah, U.; Chackalamannil, S.; Ganguly, A. K.; Chelliah, M.; Kolutuchi, S.; Beuvich, A.; McPhail, A. *J. Am. Chem. Soc.* **2006**, *128*, 12654–12655. (d) Larson, K. K.; Sarpong, R. *J. Am. Chem. Soc.* **2009**, *131*, 13244–13245. (e) Zi, W.; Yu, S.; Ma, D. *Angew. Chem., Int. Ed.* **2010**, *49*, 5887–5890.
- (8) Willis, A. C.; O'Connor, P. D.; Taylor, W. C.; Mander, L. N. *Aust. J. Chem.* **2006**, *59*, 629–632. Movassagh's synthesis of GB 13, coupled with the conversion of himandrine to GB 13 during isolation studies, provided additional evidence for revision of the Type II alkaloids.

- (9) Movassaghi, M.; Tjandra, M.; Qi, J. *J. Am. Chem. Soc.* **2009**, *131*, 9648–9650. For a synthesis of the himandrine skeleton related to the approach to GB 13 described in ref 7a, see: O'Connor, P. D.; Mander, L. N.; McLachlan, M. M. W. *Org. Lett.* **2004**, *6*, 703–706.
- (10) For an initial communication of this work, see: Evans, D. A.; Adams, D. *J. Am. Chem. Soc.* **2007**, *129*, 1048–1049.
- (11) Our view is in general agreement with that presented in ref 7b; for a biomimetic approach to himbacine as well as an alternative view on GB alkaloid biosynthesis, see ref 5e.
- (12) Claus, R. E.; Schreiber, S. L. *Organic Syntheses*; Wiley & Sons: New York, 1990; Collect. Vol. 7, pp 168–172.
- (13) For preparation of **3** and HWE procedure, see: Evans, D. A.; Miller, S. J.; Lectka, T.; von Matt, P. *J. Am. Chem. Soc.* **1999**, *121*, 7559–7573.
- (14) Evans, D. A.; Chapman, K. T.; Bisaha, J. *J. Am. Chem. Soc.* **1988**, *110*, 1238–1256.
- (15) Although *N*-benzylation is unnecessary for the completion of the synthesis, yields were optimized with *N*-benzylated material.
- (16) Dess, D. B.; Martin, J. C. *J. Am. Chem. Soc.* **1983**, *48*, 4155–4156.
- (17) Holmquist, C. R.; Roskamp, E. J. *J. Org. Chem.* **1989**, *54*, 3258–3260.
- (18) Raban, M.; Noe, E. A.; Yamamoto, G. *J. Am. Chem. Soc.* **1977**, *99*, 6527–6731.
- (19) For similar ring systems formed using aldol additions, see: Heathcock, C. H.; von Geldern, T. W. *Heterocycles* **1987**, *25*, 75–78. Alexakis, A.; Chapdlaine, M. J.; Posner, G. H. *Tetrahedron Lett.* **1978**, *44*, 4209–4212. Lohray, B. B.; Zimbiniski, R. *Tetrahedron Lett.* **1990**, *50*, 7273–7276.
- (20) Although kinetic control was desired in many cases, the thermodynamic acidity of cyclopentanone is notably greater than ethyl ketone ( $pK_a$  25.8 vs 27.1, DMSO). Bordwell, F. G.; Fried, H. E. *J. Org. Chem.* **1991**, *56*, 4218–4223.
- (21) Nicolau, K. C.; Montagnon, T.; Baran, P. S. *J. Am. Chem. Soc.* **2002**, *124*, 2245–2258.
- (22) Chackalamannil performed the conjugate addition with scandium triflate and hydrochloric acid prior to directed hydride reduction (ref 7c).
- (23) Evans, D. A.; Gage, J. R.; Leighton, J. L.; Kim, A. S. *J. Org. Chem.* **1992**, *57*, 1961–1963.
- (24) Hoffmann, R. W. *Chem. Rev.* **1989**, *89*, 1841–1860.
- (25) These conditions were used previously to effect nucleophilic displacement of allylic halides. See ref 7c and: Boyd, D. R.; Sharma, N. D.; Kerley, N. A.; McConville, G.; Allen, C. C. R.; Blacker, A. J. *ARKIVOC* **2003**, *vii*, 32–48.
- (26) Polycycle **34** differs from an advanced intermediate in Movassaghi's himandrine synthesis (ref 9) only by addition of OTBS at C13.
- (27) Protonation likely occurs via trace acid present in *d*-chloroform.
- (28) Page, M. I.; Jencks, W. P. *Proc. Natl. Acad. Sci. U.S.A.* **1971**, *68*, 1678–1683.
- (29) Maple, S. R.; Allerhand, A. *J. Am. Chem. Soc.* **1987**, *109*, 6609–6614.
- (30) An analogous intramolecular aldol addition, cyclization of 2,6-heptanedione to 3-hydroxy-3-methylcyclohexanone, is substantially exergonic ( $\Delta G = -2.4$  kcal/mol), suggesting that intramolecularity can increase the favorability of an aldol process by 5–6 kcal/mol. Guthrie, J. P.; Guo, J. *J. Am. Chem. Soc.* **1996**, *118*, 11472–11487.
- (31) Energies given for eqs 5–7 were computed using the CBS-QB3 method with SMD solvation (THF). (a) CBS-QB3: Montgomery, J. A., Jr.; Frisch, M. J.; Ochterski, J. W.; Petersson, G. A. *J. Chem. Phys.* **1999**, *110*, 2822–2827. (b) SMD solvation: Marenich, A. V.; Cramer, C. J.; Truhlar, D. G. *J. Phys. Chem. B.* **2009**, *113*, 6378–6396.
- (32) Candidate structures were generated using molecular mechanics and optimized further at M06-2X/6-31g with SMD implicit solvation. All energies are given as single-point electronic energies at M06-2X/6-311+g(d,p) with M06-2X/6-31g(d) geometries and free energy corrections (298 K). In model systems whose energies could be accurately estimated by CBS-QB3, M06-2X was shown to perform the best of a variety of density functional methods. See Supporting Information for details. M06-2X has been shown to outperform the commonly used B3LYP basis set for branched alkanes and for  $\pi$  to  $\sigma$  bond transitions, in part due to a fortuitous cancellation of errors: (a) Song, J.-W.; Tsuneda, T.; Sato, T.; Hirao, K. *Org. Lett.* **2010**, *12*, 1440–1443. (b) Pieniazek, S. N.; Clemente, F. R.; Houk, K. N. *Angew. Chem., Int. Ed.* **2008**, *47*, 7746–7749. (c) Wheeler, S. E.; Moran, A.; Pieniazek, S. N.; Houk, K. N. *J. Phys. Chem. A* **2009**, *113*, 10376.
- (33) Tautomeric enamines and en ammonium ions were found to be 6–13 kcal/mol higher in energy and were not considered further.
- (34) Movassaghi, M.; Chen, B. *Angew. Chem., Int. Ed.* **2006**, *45*, 565–568.
- (35) Howells, D. M.; Barker, S. M.; Watson, F. C.; Light, M. E.; Hursthouse, M. B.; Kilburn, J. D. *Org. Lett.* **2004**, *6*, 1943. See Supporting Information for comparison with computed structures.
- (36) Bahmanyar, S.; Houk, K. N. *J. Am. Chem. Soc.* **2001**, *123*, 11273–11283.
- (37) Modeling of one explicit methanol molecule in a variety of orientations provided transition states of comparable energy (see Supporting Information).